Turk J Phys
28 (2004) , 391 – 396.

Structural Characterization and Magnetization of $Mg_{0.5}Cu_{0.5}Y_xFe_{2-x}O_4$ Ferrites

Mansour AL-HAJ
Physics Department, Mutah University, Mutah, JORDAN
e-mail: Mansour@mutah.edu.jo

Received 22.07.2004

Abstract

$Mg_{0.5}Cu_{0.5}Y_xFe_{2-x}O_4$ ferrites were prepared by the solid state reaction method and were characterized by X-ray diffraction and magnetization measurements. A single spinel phase was obtained in the range $0 \leq x \leq 0.08$. The lattice parameter was found to increase with the increase of x except at $x = 0.08$, which may indicate a distortion in the spinel lattice. The saturation magnetization was found to decrease with increasing x due to replacement of the magnetic Fe^{3+} ions by the nonmagnetic Y^{3+} ions.

Key Words: Ferrites; X-ray diffraction; lattice parameter; X-ray density; magnetization.

1. Introduction

Ferrites are an important class of magnetic materials which have many applications, including use as humidity sensors [1] and green anode materials [2]. The spinel ferrites can be described by the formula $(M_{1-\gamma}\ Fe_\gamma)\ [M_\gamma\ Fe_{2-\gamma}]\ O_4$, where M is a divalent element, the round and square brackets denote tetrahedral and octahedral sites of co-ordination, respectively, and γ is the inversion parameter whose value is in the range $0 \leq \gamma \leq 1$. For example, the ferrite $ZnFe_2O_4$ has $\gamma = 0$ and is a normal spinel at room temperature, while the ferrite $NiFe_2O_4$ has $\gamma = 1$ and is an inverse spinel.

The physical properties of ferrites are dependent on several factors, such as preparation method, sintering process [3] and constituent elements. Several methods can be used to prepare ferrites, such as solid state reaction, mechanical milling, reverse micelle and citrate precursor [4]. The effect of various substituting cations on the structural, electrical, dielectric and magnetic properties of ferrites was the subject of an extensive research work [5–20] which used techniques such as X-ray and neutron diffraction, thermal analysis, Mössbauer spectroscopy, magnetization and electrical conductivity.

The main aim of the present work is to study the influence of yttrium ions on the structure and magnetization of $Mg_{0.5}Cu_{0.5}Y_xFe_{2-x}O_4$ ferrites, with $x = 0$, 0.02, 0.04, 0.06, 0.08 and 0.1.

2. Experimental Procedure

The ferrite powders were prepared by the usual ceramic method. Analytical grade oxides (MgO, CuO, Fe_2O_3, Y_2O_3) were mixed, ground and sintered at 1100 °C in a Carbolite furnace for 10 h. Each sample was then cooled slowly to room temperature, ground and sintered again at 1100 °C for 10 h. The X-ray diffraction (XRD) patterns were taken using a Seifert 3003 TT diffractometer operating at 40 kV and 40

mA. The experimental setup is: Cu source / Ni filter / 3 mm slit / primary collimator / 2 mm slit / sample / 4 mm slit / secondary collimator / 0.1 mm slit / detector. The diffractometer was calibrated using a standard Si powder. The samples were scanned were scanned in steps of 0.01° and the measuring time is 1 s. The magnetization measurements were done on samples of equal masses at room temperature using a 9600 LDJ vibrating sample magnetometer.

3. Results and Discussion

To determine the cationic distribution of $Mg_{0.5}Cu_{0.5}Fe_2O_4$ ferrite, the program AutoQuan was used to perform a Rietveld refinement of the XRD pattern [21]. The method is an optimization procedure to fit a model of the examined sample to the measured diffraction pattern. A parameter set is used for fitting. The model is refined by minimizing, by a least-squares process, the residual

$$\sum_i w_i(y_i - y_{ic})^2, \tag{1}$$

where $w_i = y_i^{-1}$ is a weight for the i^{th} measuring point, y_i is the measured counts of the i^{th} point and y_{ic} is the calculated counts of the i^{th} point. y_{ic} is the sum of the contributions from all Bragg reflections k of the sample:

$$y_{ic} = y_{ib} + S\sum_k P_k m_k L_k T_k |F_k|^2, \tag{2}$$

where y_{ib} is the background of the i^{th} point, S is a scale factor, P_k is the profile function, m_k is the multiplicity of the reflection k, L_k is the Lorentz polarization factor, T_k is the isotropic Debye-Waller factor for thermal diffuse scattering spread and F_k is the structure factor.

The background y_{ib} is fitted by a polynomial whose order is determined automatically. The preferred orientation is modeled by the mathematical model of spherical harmonics. The profile function is taken as a convolution of the wavelength distribution, the geometry function and the sample function. A Lorentzian function is taken for the sample function:

$$L_1 = \frac{1}{\pi} \cdot \frac{b_1}{b_1^2 + (x - x_0)^2}, \tag{3}$$

where x_0 is the peak position and b_1 is the reflection broadening parameter due to crystalline size. The influence of microstrains is considered by folding a Lorentzian function with a squared Lorentzian function:

$$L_{12} = L_1 * L_2, \tag{4}$$

where

$$L_2 = \frac{2}{\pi} \cdot \frac{b_2^3}{[b_2^2 + (x - x_0)^2]^2}, \tag{5}$$

where b_2 is the reflection broadening parameter due to microstrains and crystalline size distribution.

The agreement between the observations and the model is indicated by the goodness of fit:

$$GOF = \frac{\sum_i w_i(y_i - y_{ic})^2}{N - P}, \tag{6}$$

where N and P are the number of profile points and refined parameters, respectively; GOF should approach the ideal value of unity.

Figure 1 shows the graphical representation of the measured XRD values, calculated diagram, background (top part of the figure), and the difference curve (bottom part of the figure) for the $Mg_{0.5}Cu_{0.5}Fe_2O_4$ ferrite. The structural model was taken as the spinel phase with the space group $Fd\bar{3}m$. The refined parameters such as the lattice and atomic parameters were adjusted until a value of 1.0016 was obtained for the GOF. It should be mentioned that this fit was obtained by assuming that all the Mg^{2+} and Cu^{2+}ions are occupying octahedral sites, so that the cationic distribution is (Fe^{3+}) $[Mg^{2+}_{0.25}$ $Cu^{2+}_{0.25}$ $Fe^{3+}_{0.5}]_2$ O_4 and the inversion parameter $\gamma = 1$. This means that 50% of the octahedral sites are occupied by the Mg^{2+} and Cu^{2+} ions and the other 50% are occupied by Fe^{3+} ions.

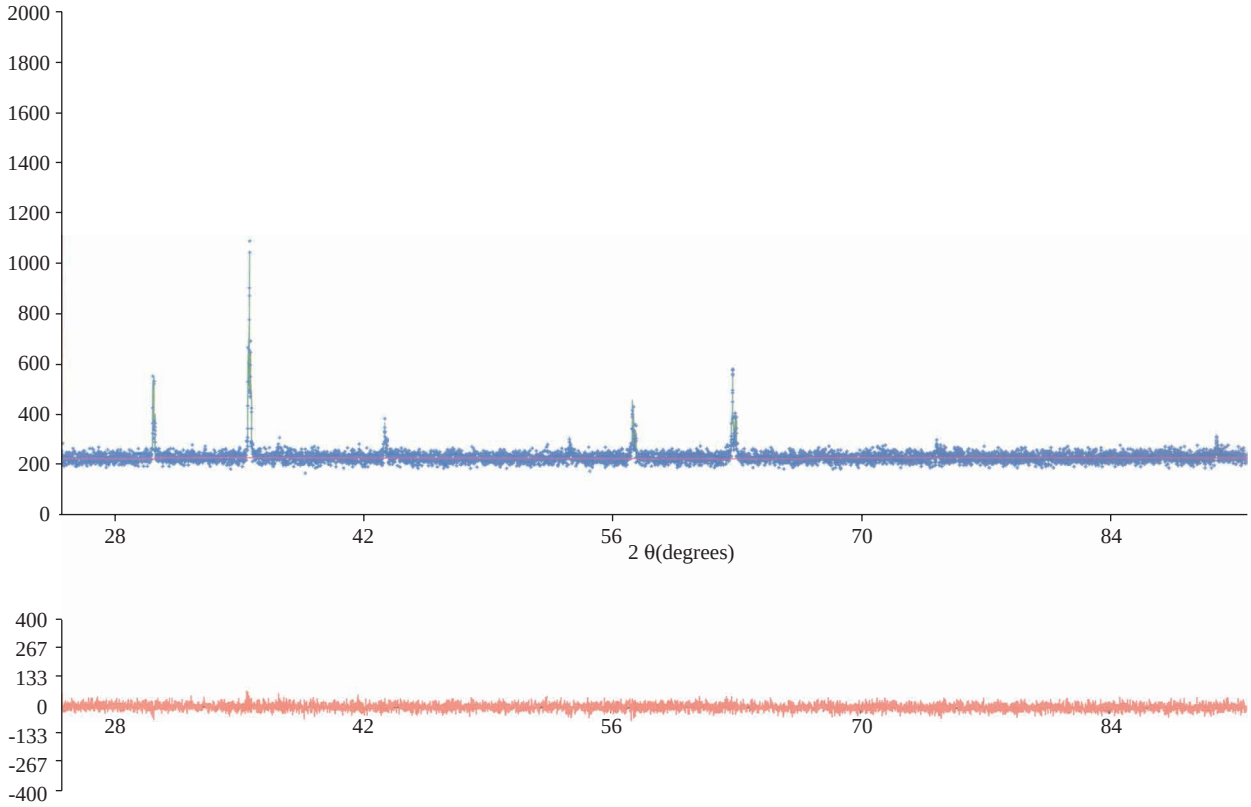

Figure 1. Graphical representation of the measured XRD values, calculated diagram, background and the difference curve for $Mg_{0.5}Cu_{0.5}Fe_2O_4$ ferrite.

The single spinel phase was obtained for all $Mg_{0.5}Cu_{0.5}Y_xFe_{2-x}O_4$, except for $x = 0.1$. Selected XRD patterns are shown in Figure 2. The reflection peak indicated by arrow in Figure 2c is a reflection peak from the phase $YO_{1.401}$.

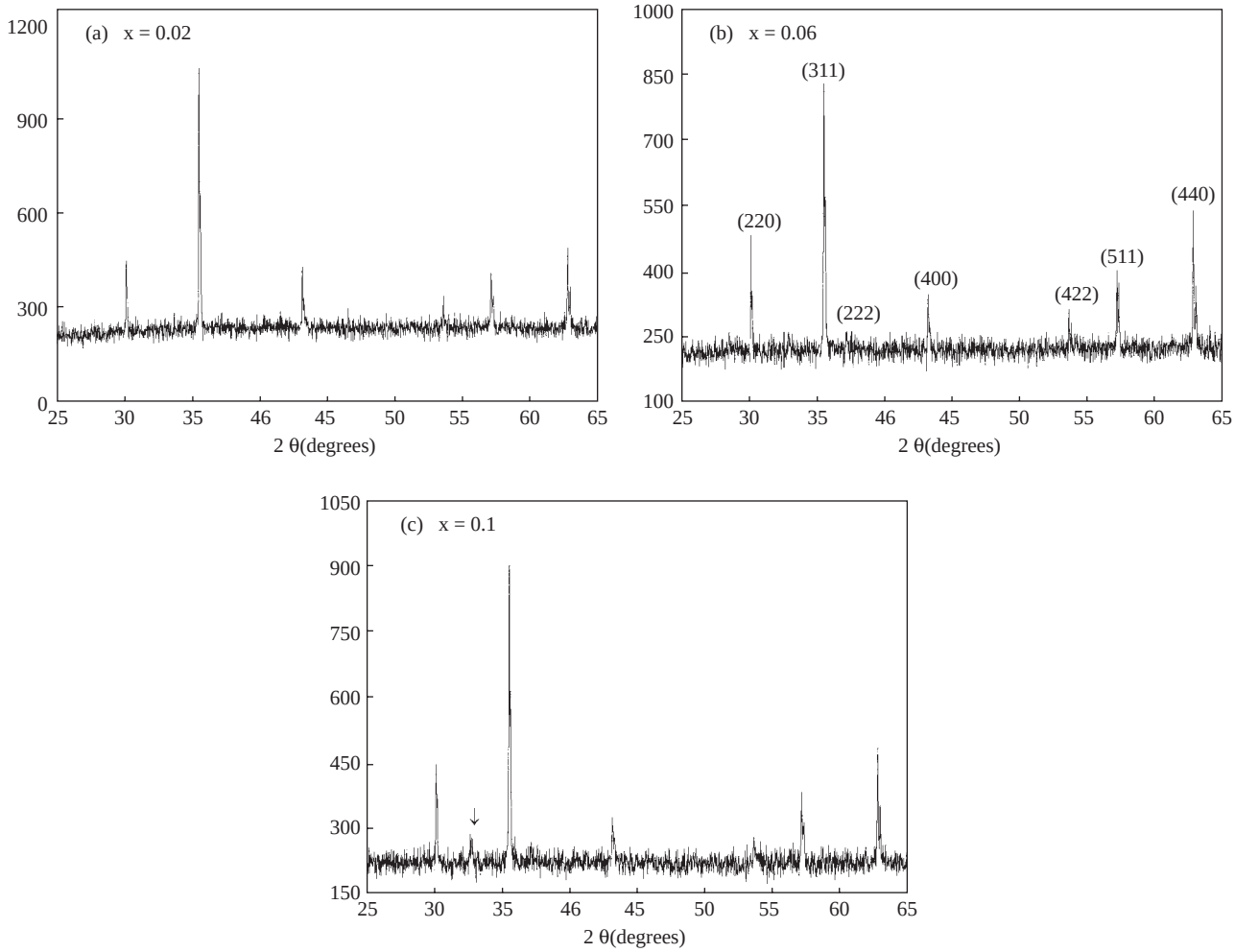

Figure 2. The XRD patterns for selected samples.

It is known that the replacement of cations by larger ones in the spinel lattice causes an increase in the lattice parameter, as is the case for example in $Cd_{1-x}Co_xFe_2O_4$ ferrites [6]. Figure 3a shows the dependence of the lattice parameter a on the Y^{3+} content x. The lattice parameter increases with the increase of x, except at the critical value $x = 0.08$, where a decrease in the lattice parameter is observed. The increase of a between $x = 0$ and $x = 0.06$ is due to the replacement of Fe^{3+} ions (radius = 0.64 Å) by the larger Y^{3+} ions (radius = 0.90 Å) at the octahedral sites. The decrease of a at $x = 0.08$ is probably due to a distortion in the spinel lattice because of the relatively high radius of Y^{3+}. This is evidenced by the appearance of yttrium oxide at $x = 0.1$, besides the spinel phase. Therefore, a single spinel phase cannot be obtained at $x \geq 0.1$.

The X-ray density was calculated using the equation:

$$d_x = \frac{8M}{N_A a^3}, \tag{7}$$

where M is the molar mass of the ferrite, a is the lattice parameter and N_A is Avogadro's number. The dependence of d_x on x is shown in Figure 3b. It is revealed that d_x increases with the increase of x up to $x = 0.08$, since Fe^{3+} ions are being replaced by the larger mass Y^{3+} ions. At $x = 0.1$, the value of d_x is decreased due to formation of the phase $YO_{1.401}$ in addition to the spinel phase. Therefore, an agreement between the results obtained from the behavior of a and d_x can be seen.

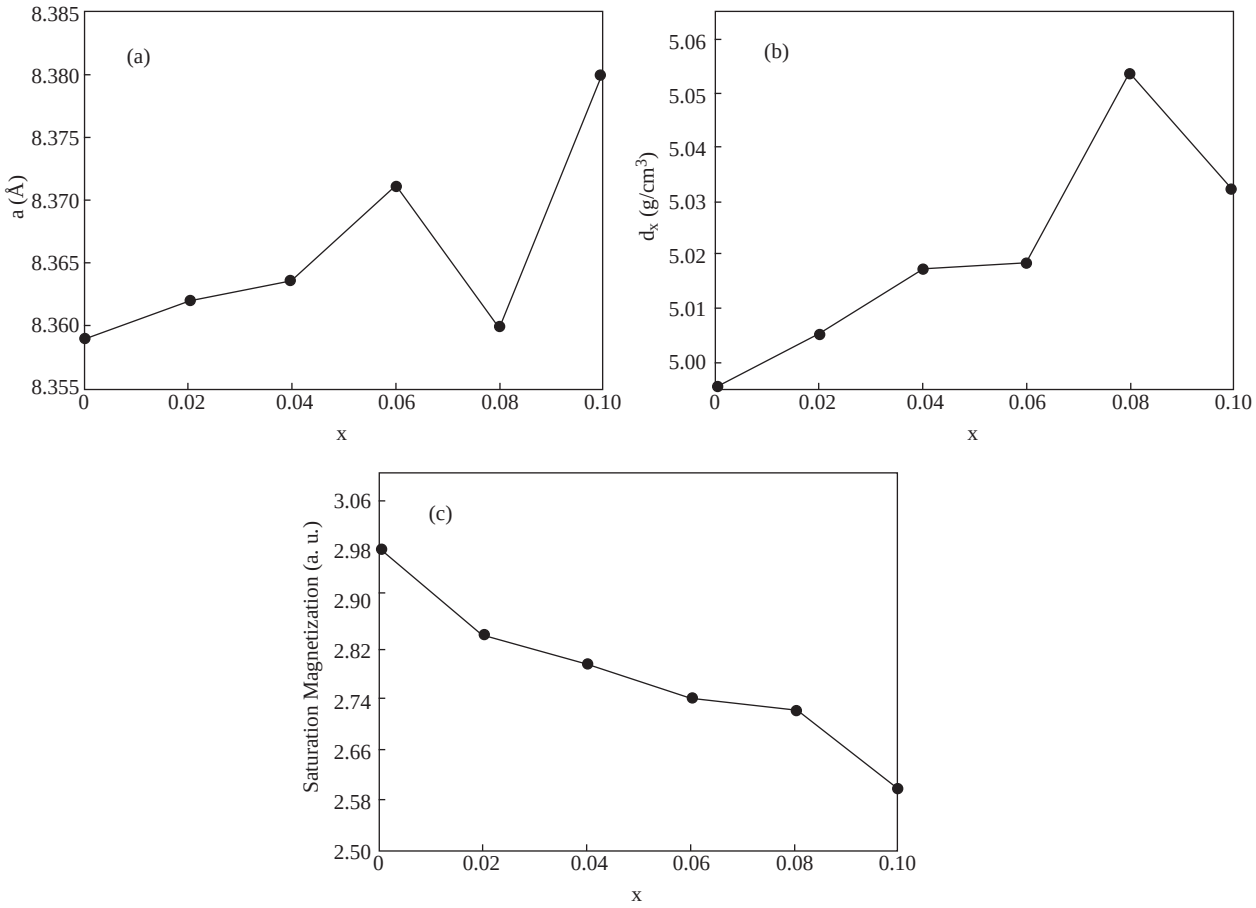

Figure 3. The dependence of the lattice parameter (a), the X-ray density (b) and the saturation magnetization (c) on the Y^{3+} content.

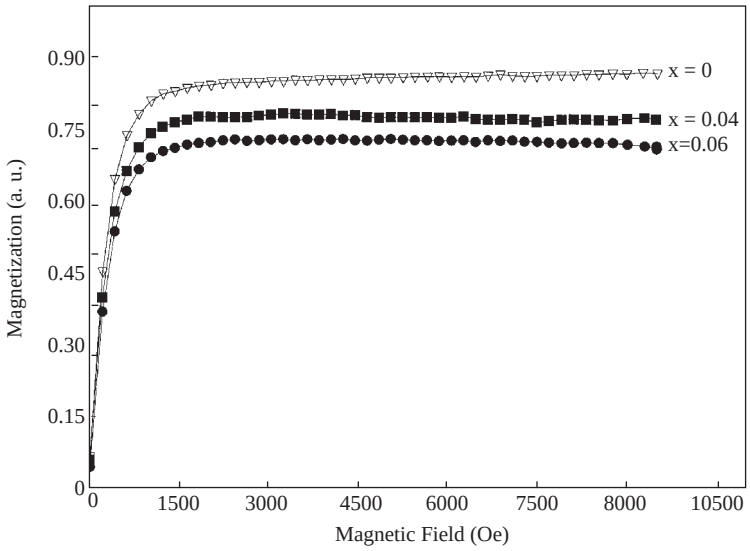

Figure 4. The magnetization versus magnetic field curves for selected samples.

The magnetization versus magnetic field curves for selected samples are shown in Figure 4. All samples

are ferromagnetic at room temperature. The saturation magnetization as a function of x is shown in Figure 3c. It is seen that the saturation magnetization decreases as x is increased due to the replacement of the magnetic Fe^{3+} ions by the nonmagnetic Y^{3+} ions. The major decrease of saturation magnetization at $x = 0.1$, compared with the other Y^{3+} containing samples, is probably due to the formation of the intermetallic phase $YO_{1.401}$ which degrades the magnetic properties.

4. Conclusions

(1) A single spinel phase was obtained for $Mg_{0.5}Cu_{0.5}Y_xFe_{2-x}O_4$ ferrites in the Y^{3+} content range $0 \leq x \leq 0.08$.

(2) The lattice parameter increases as the Y^{3+} content is increased except at $x = 0.08$, which may indicate a distortion in the spinel lattice at this value of x.

(3) The saturation magnetization decreases as the Y^{3+} content is increased, due to the replacement of the magnetic Fe^{3+} ions by the nonmagnetic Y^{3+} ions.

References

[1] N. Rezlescu, E. Rezlescu, C. Sava, F. Tudorache and P. Popa, *Phys. Stat. Sol.* (a), **201,** (2004), 17.

[2] L. John Berchmans, R. Kalai Selvan and C. Augustin, *Mater. Lett.*, **58**, (2004), 1928.

[3] P. Yadoji, R. Peelamedu, D. Agrawal and R. Roy, *Mater. Sci. Eng.* B, **98**, (2003), 269.

[4] A. Singh, T. Goel and R. Mendiratta, *Phys. Stat. Sol.* (a), **201**, (2004), 1453.

[5] K. Modi, J. Gajera, M. Chhantbar, K. Saija, G. Baldha and H. Joshi, *Mater. Lett.*, **57**, (2003), 4049.

[6] M. Gabal and S. Ata-Allah, *Mater. Chem. Phys.*, **85**, (2004), 104.

[7] R. Bhowmik, R. Ranganathan, S. Sarkar, C. Bansal and R. Nagarajan, *Phys. Rev.* B, **68**, (2003), 134433.

[8] M. Ahmed, N. Okasha and M. Gabal, *Mater. Chem. Phys.*, **83**, (2004), 107.

[9] A. Singh, T. Goel and R. Mendiratta, *Jpn J. Appl. Phys.*, **42**, (2003), 2690.

[10] M. Fayek and S. Ata-Allah, *Phys. Stat. Sol.* (a), **198**, (2003, 457.

[11] M. Mahmoud, A. Abdallas, H. Hamdeh, W. Hikal, S. Taher and J. Ho, *J. Magn. Magn. Mater.*, **263**, (2003), 269.

[12] S. Bid and S. Pradhan, *Mater. Chem. Phys.*, **82**, (2003), 27.

[13] H. Ehrhardt, S. Campbell and M. Hofmann, *Scripta Mater.*, **48**, (2003), 1141.

[14] N. Okasha, *Mater. Chem. Phys.*, **84**, (2004), 63.

[15] K. Kumar, A. Reddy and D. Ravinder, *J. Magn. Magn. Mater.*, **263**, (2003), 121.

[16] A. Al-Rawas, A. Rais, A. Yousif, A. Gismelseed, M. Elzain, S. Mazen and A. Al-Falaky, *J. Magn. Magn. Mater.*, **269**, (2004), 168.

[17] A. Sattar and S. Rahman, *Phys. Stat. Sol.* (a), **200**, (2003), 415.

[18] M. Ahmed, N. Okasha and L. Salah, *J. Magn. Magn. Mater.*, **264**, (2003), 241.

[19] Z. Yue, J. Zhou, Z. Gui and L. Li, *J. Magn. Magn. Mater.*, **264**, (2003), 258.

[20] A. El-Sayed, *Mater. Chem. Phys.*, **82**, (2003), 583.

[21] Seifert Analytical X-ray, AutoQuan, version 2.62, 2002.